Applied Catalysis A: General 391 (2011) 436–442

Contents lists available at ScienceDirect

Applied Catalysis A: General

journal homepage: www.elsevier.com/locate/apcata

Accelerated cellulose depolymerization catalyzed by paired metal chlorides in ionic liquid solvent

Yu Su, Heather M. Brown, Guosheng Li, Xiao-dong Zhou, James E. Amonette, John L. Fulton, Donald M. Camaioni, Z. Conrad Zhang*

Pacific Northwest National Laboratory, Institute for Interfacial Catalysis, P.O. Box 999, Richland, WA 99352, United States

ARTICLE INFO

Article history:
Received 2 March 2010
Received in revised form 24 August 2010
Accepted 23 September 2010
Available online 1 November 2010

Keywords:
Ionic liquid
1-Alkyl-3-methylimidazolium chloride
1-Ethyl-3-methyl-imidazolium chloride
Cellulose
Biomass
Depolymerization
Catalysis
Bioenergy
Hydrolysis
Glucose
Cellobiose
Maltose
Cellulose conversion
Catalyst
Paired metal chlorides
$CuCl_2$
$PdCl_2$

ABSTRACT

Efficient hydrolytic depolymerization of crystalline cellulose to sugars is a critical step and has been a major barrier for improved economics in the utilization of cellulosic biomass. A novel catalytic system involving $CuCl_2$ (primary metal chloride) paired with a second metal chloride, such as $CrCl_2$, $PdCl_2$, $CrCl_3$ or $FeCl_3$ in 1-ethyl-3-methylimidazolium chloride ([EMIM]Cl) ionic liquid solvent has been found to substantially accelerate the rate of cellulose depolymerization under mild conditions. These paired metal chlorides are particularly active for the hydrolytic cleavage of 1,4-glucosidic bonds when compared to the rates of acid-catalyzed hydrolysis at similar temperatures (80–120 °C). In contrast, single metal chlorides with the same total molar loading showed much lower activity under similar conditions. Experimental results illustrate the dramatic effect of the second metal chloride in the paired catalytic system. An array of characterization techniques, including electron paramagnetic resonance (EPR) spectroscopy, differential scanning calorimetry (DSC), X-ray absorption fine structure (XAFS) spectroscopy, and X-ray absorption near edge structure (XANES) spectroscopy, in combination with theoretical calculations at the DFT level, was used to reveal a preliminary understanding of possible mechanisms involved in the paired $CuCl_2/PdCl_2$ catalytic system. We discovered that Cu(II) was reduced during the course of the reaction to Cu(I) only in the presence of a second metal chloride and a carbohydrate source such as cellulose in the ionic liquid system. Our results suggest that Cu(II) generates protons by hydrolysis of water to catalyze the depolymerization step, and serves to regenerate Pd(II) reduced to Pd(0) by side reactions. Pd(II) likely facilitates the depolymerization step by coordinating the catalytic protons, and also promotes the formation of hydroxymethylfurfural (HMF). Our results also suggest that the C2-proton of the imidazolium ring is not activated by the paired metal-chloride catalysts.

1. Introduction

Cellulose is nature's most abundant polymer that stores energy in chemical bonds derived from CO_2 and H_2O by photosynthesis. Its chemical structure is made of anhydro-glucose linearly linked by β-1,4-glucosidic bonds. An extensive network of such polymer chains via hydrogen-bonding [1] and van der Waals forces [2] arranges in ordered alignment, resulting in a supramolecular cellulose structure of various size, crystallinity, and complexity, depending on the type of biomass. Decrystallization and hydrolytic cleavage of cellulose polymers to glucose has been a bottleneck in the path toward energy-efficient and economical utilization of cellulosic biomass. Considerable research has focused on improving the rate of cellulose hydrolysis to produce the constituent sugars. The two most studied cellulose depolymerization processes in aqueous systems involve either multiple enzymes [3] or strong mineral acids [4] as catalysts. However progress has been limited partly due to the lack of solubility of cellulose in water. Enzymatic hydrolysis of cellulose is typically slow and the rate is also inhibited by contaminants originating from other biomass components. Pretreatment of cellulose, for example by ammonia in a high-pressure process or by mechanical milling, is typically required to increase the accessible surface area of cellulose for a reasonable rate of enzymatic hydrolysis [5]. Mineral acids have been used to catalyze hydrolysis at a variety of acid concentrations and temperatures. However, a rather high temperature (180–230 °C) is needed to obtain an acceptable rate of cellulose hydrolysis using only a dilute acid [6]. Degradation of the resulting glucose becomes an issue at this temperature.

Taking advantage of the ability of 1-alkyl-3-methylimidazolium chloride, [AMIM]Cl, ionic liquids to dissolve cellulose [7,8], we evaluated a large number of metal chlorides, in catalytic amounts, dissolved in the same media [9]. We recently reported that, in

* Corresponding author. Tel.: +1 713 299 4165; fax: +1 281 334 2832.
E-mail addresses: zczhang@yahoo.com, conrad.zhang@kior.com (Z.C. Zhang).

0926-860X/$ – see front matter © 2010 Elsevier B.V. All rights reserved.
doi:10.1016/j.apcata.2010.09.021

the $CuCl_2/CrCl_2$ system, tuning the $CuCl_2/CrCl_2$ ratio allowed us to identify the conditions for optimal rate of cellulose hydrolysis to monocarbohydrate sugars, and for optimal yield to 5-hydroxymethylfurfural [10]. Here, we report results from the $CuCl_2/PdCl_2$ catalyst system in 1-ethyl-3-methylimidazolium chloride, [EMIM]Cl, that not only considerably accelerates the rate of cellulose hydrolytic depolymerization over single $CuCl_2$ or $PdCl_2$ to glucose under mild conditions, but also allows us to apply a combination of physical techniques to study the mechanism of the unique paired metal chloride catalysts in the ionic liquid solvent with reduced complexity as compared to the $CuCl_2/CrCl_2$ system.

2. Experimental

2.1. Sample preparation and catalytic reactions

A special high purity 1-ethyl-3-methylimidazolium chloride ([EMIM]Cl, 99%) was purchased from Solvent-Innovation (Cologne, Germany, Lot No. 99/972). $CuCl_2$ (99.9%), $PdCl_2$ (99.9%), cellobiose, and cellulose (Cellulose, cotton linters, product no. C6663) were obtained from Sigma–Aldrich (St. Louis, MO, USA).

In a standard experiment, 500 mg [EMIM]Cl with catalyst was loaded into nominal 4-mL vials (15.5 mm diameter × 50 mm tall). The catalyst consisted of either $CuCl_2$, $PdCl_2$, or paired $CuCl_2/PdCl_2$, and, unless otherwise specified, was present at a total concentration of 6 mol% with respect to the glucose concentration calculated from the cellulose feed. The vials were sealed and inserted into a high-throughput batch reactor (Symyx Technologies, Inc., Sunnyvale, CA), where they were heated to 150 °C and shaken at 600 rpm for 30 min. After the reactor had cooled to room temperature, 50 mg cellulose (10 wt.% with respect to ionic liquid) was added to each vial. The vials were sealed and reinserted into the high-throughput reactor. During the dissolution process, the vials were heated to 100 °C or 120 °C and shaken at 600 rpm for 1 h. Then the reactor was cooled to room temperature, and 50 μl H_2O which is near ten times excess over a stoichiometric amount required for full hydrolysis of the cellulose feed, was added to each vial to initiate the depolymerization. The vials were sealed and reinserted into the high-throughput reactor at 80, 100, or 120 °C for a specified time period and shaken at 600 rpm. Exactly 2 ml of water was consequently added to each vial after the reactor had cooled to room temperature. The vials were sealed and centrifuged at 2000 rpm for 30 min. A single liquid layer was formed and the liquid products were analyzed by HPLC. All results were replicated at least 5 times.

For catalyst characterization by EPR and XAFS spectroscopies, we used cellobiose, which has the same characteristic β-1,4-glucosidic bond as in cellulose, in [EMIM]Cl to study paired metal chlorides and their properties.

2.2. Differential scanning calorimetry

Differential scanning calorimetry (DSC) experiments were conducted on a Perkin Elmer Pyris 6 instrument. All the catalyst–ionic liquid mixtures investigated ($CuCl_2$, $PdCl_2$, and $CuCl_2$–$PdCl_2$) were prepared with constant catalyst loading by the same standard experimental procedure described above. A small amount of each sample (about 20 mg) was then added into a 50 μl aluminum pan (0.1 mm × 2.1 mm) and sealed it with a 30 μl aluminum pan (0.1 mm × 2.1 mm) as the lid by a Universal Sealing Press (Perkin Elmer) inside a glove box. The sealed sample was analyzed by DSC test using the identical empty pans (sealed in the same manner) as the blank. During each run, the sample was heated to 180 °C with a heating rate of 5 °C/min. For samples containing cellulose, 10 wt.% cellulose was added to each prepared catalyst–ionic liquid mixture and subsequently moved to a batch reactor. The reactor was heated to 150 °C for 20 min and cooled to room temperature. The prepared samples were then weighed and sealed by the same process described above before being analyzed by DSC. All the sample weighing and the subsequent sealing process were conducted under dry nitrogen in a controlled atmosphere chamber to prevent exposure of the samples to air and moisture. Each catalyst–ionic liquid mixture was tested several times and the results obtained were reproducible.

2.3. Electron paramagnetic resonance spectroscopy

In situ electron paramagnetic resonance (EPR) spectra were collected using a Bruker ELEXSYS E500 X-band spectrometer operated in continuous-wave mode. Ionic-liquid samples were injected into a variable-temperature liquid flat cell (Wilmad, WG-865-B-Q), which was then capped and mounted in a TE102 cavity (Bruker, ST9404). The temperature of the sample in the flat cell was controlled by a flow of air heated to appropriate temperature and measured by a thermocouple (*K* type). The *g* factors of the ionic liquid samples were calibrated using a standard powder sample DPPH (α,α′-diphenyl-β-picryl hydrazyl), which has a *g* factor of 2.0036 ± 0.0003 [11]. Typical operating parameters include microwave frequency 9.367 GHz; modulation frequency 32 kHz; modulation amplitude 16.6; receiver gain 70 dB; and microwave power ~12.5 mW.

2.4. X-ray absorption fine structure spectroscopy

The Pd (24,352.6 eV) and Cu (8980.5 eV) K-edge XAFS spectra were collected in transmission mode on the bending magnet beamline (PNC-CAT, Sector 20) at the Advanced Photon Source, Argonne National Laboratory. The bending magnet beamline was chosen over the much higher flux insertion-device line to minimize the potential for beam damage to the Cu chemistry. There was no evidence of beam-induced reduction of Cu(II) to either Cu(I) or Cu(0). The XANES spectrum of the Cu(I) in solution taken for 1 min was identical to spectra that were acquired after 1 h of exposure to the beam. A 1 mm × 3 mm beam with a flux of 5×10^{10} photons s^{-1} was used for Cu XAFS.

The Pd XAFS of the [EMIM]Cl solutions was measured in 1.5 cm × 6 cm polyethylene bottles. The bottles were placed in a vertical position in a heated sample holder to provide a 1.5 cm pathlength for the X-ray beam. The Cu XAFS was acquired in a container constructed from a 1 mm thick PEEK spacer that defined the beam pathlength. Two thin Kapton films were affixed to this spacer to provide for beam transmission.

We used standard methods to analyze the XAFS data [12], using portions of the UWXAFS program [13]. The XAFS oscillations, $\chi(k)$, were extracted from the experimentally measured absorption coefficient using an automated background subtraction method (AUTOBK) developed by Newville et al. [14]. The photoelectron amplitude, phase and mean-free-path factors were derived from theoretical standards calculated by FEFF8 [15]. The fitting of the FEFF8 theoretical standards to the experimental data was accomplished using an analysis program (FEFFIT) [16].

Pd and Cu standard compounds were used to establish the value of the core hole factor, S_0^2. We used a core-hole factor of $S_0^2 = 0.76$ and 0.85 for Pd and Cu, respectively. The XAFS $\chi(k)$ data were weighted by k^2, and windowed between $2.0 < k < 18.0$ Å^{-1} using a Hanning window with $dk = 1.0$ Å^{-1}. The fits were done to both the real and imaginary parts of $\tilde{\chi}(R)$ in the region of $1.0 < R < 5.5$ Å. Quality of fits was evaluated using the criteria defined in FEFFIT, the automated software for fitting the structural parameters.

The XAFS peaks are broadened and shifted from their true positions due to the photoelectron phase shift but the actual positions and distributions are recovered upon fitting to theory. The signifi-

cant photoelectron multiple scattering peaks between 3.2 and 4.3 Å were used to confirm the square planar geometry of the $PdCl_4^{2-}$ complex and the slightly bent collinear geometry of the $CuCl_2^-$ complex after *in situ* reaction at 100 °C.

2.5. Computational methods

Electronic structure calculations were performed using the NWChem suite of programs [17]. Minimum energy structures were optimized using Density Functional Theory [18,19], the B3LYP functional [20] and the 6-31G** basis set with added diffuse s and p functions on Cl and diffuse s, p, and d functions on Cu. Repeat calculations using the Ahlrichs TZV basis set [21] for Cu and Cl with Ahlrichs polarization functions yielded similar geometrical parameters for Cu and Cl (e.g., 2.176 Å vs. 2.157 Å, and 180° bond angle for $CuCl_2^-$). Frequency calculations showed the absence of imaginary vibrational modes.

3. Results and discussion

Unless otherwise specified, the total metal-chloride loading was maintained at 37 μmol per gram of [EMIM]Cl solvent, corresponding to 6 mol% with respect to the calculated glucose-monomer concentration based on the cellulose feed. At this total metal chloride loading, the molar ratio of metal chloride to [EMIM]Cl solvent is 0.005. We first dissolved each metal-chloride catalyst in the solvent to obtain a homogeneous solution. We then added cellulose to this solution and allowed it to decrystallize (i.e., dissolve) at a specified swelling temperature (100–120 °C) for 30 or 60 min. Lastly, we initiated depolymerization and the subsequent conversion of glucose by adding 10 wt.% water at a specified low reaction temperature (100–120 °C). The upper limit of 120 °C was selected to minimize degradation of glucose and its derivatives.

Because degradation of glucose and derivative products by the metal chloride catalysts in the [EMIM] solvent becomes serious at temperatures above 120 °C [22] the experiments for cellulose hydrolysis were conducted in a temperature range of 80–120 °C. In preliminary experiments, a number of pure metal chlorides, $CuCl_2$, $CrCl_2$, $CrCl_3$, $PdCl_2$, $FeCl_3$, etc. were evaluated in the [EMIM]Cl solvent; no single metal chloride was found to have meaningful activity for the reaction at this low temperature range [10]. In this work, we focus on the results obtained from the $CuCl_2$, $PdCl_2$, and the paired $CuCl_2/PdCl_2$ systems in the solvent as described in Section 2. For the paired $CuCl_2/PdCl_2$ catalysts, the $CuCl_2/PdCl_2$ ratio was varied while the total molar loading was unchanged.

We conducted a series of depolymerization experiments with two metal chlorides, $CuCl_2$ and $PdCl_2$, in which the total loading was kept at 37 μmol/g [EMIM]Cl, while the relative proportions of the two metals varied from a Cu mole fraction (χ_{CuCl_2}) of 0–1. For these experiments, the cellulose was dissolved in [EMIM]Cl at 100 °C for 1 h before adding water and raising the reaction temperature to 120 °C. After 1 h of reaction, very low activity (total product yield <10%) for cellulose hydrolysis was seen for the end member solutions containing a single metal chloride (i.e., $\chi_{CuCl_2} = 0$ or 1, Fig. 1). In strong contrast, mixtures of the two metal chlorides consistently resulted in higher total product yields [as high as 73% ($\chi_{CuCl_2} = 0.83$)]. The results are comparable to those obtained with the $CuCl_2/CrCl_2$ mixture [10]. The most active range was for mixtures containing more Cu than Pd (i.e., χ_{CuCl_2} of 0.5–0.9) under the specified reaction conditions and reaction time. In these experiments, glucose was the major product, along with lower yields of cellobiose and HMF. The presence of cellobiose suggests that higher saccharide oligomers, such as cellotriose and cellotetraose, also may be present, although not analytically quantified. These higher saccharide oligomers would be expected to contribute to the unaccounted species in the mass balance calculation.

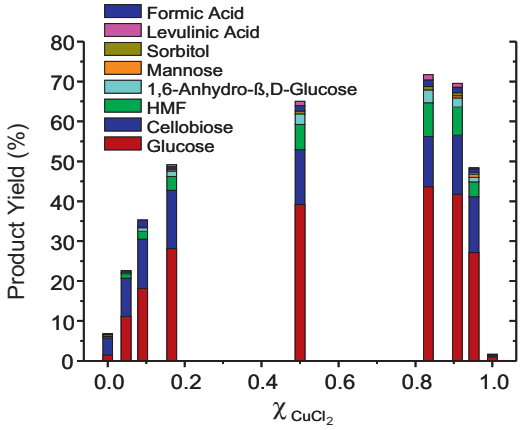

Fig. 1. Hydrolysis product yield from cellulose using paired $CuCl_2$ and $PdCl_2$ catalysts with varying χ_{CuCl_2} from 0 to 1 at 120 °C for 0.5 h. The cellulose was swelled in [EMIM]Cl at 100 °C for 1 h before adding the catalyst. Total metal chloride loading is 37 μmol/g [EMIM]Cl (6 mol% with respect to the glucose units present in the cellulose feed).

Insignificant amounts (<10%) of glucose were obtained for mixtures of $PdCl_2$ with other metal chlorides such as $CrCl_2$ and $FeCl_3$, suggesting that the $CuCl_2$ as a primary metal chloride is essential for the observed synergy in paired metal chlorides. A single metal chloride, even at much higher total loadings, was found to be ineffective for the desired cellulose depolymerization. We also assessed the importance of the Lewis acidity for the reaction. It was found that $AlCl_3$, a known strong Lewis acid, was not effective. Lastly, H_2SO_4 and HCl at a concentration equivalent to the total metal-chloride molar loading was also found to be less active than the paired metal chlorides under similar conditions (in about 30% of the yield).

In a separate study involving paired $CuCl_2$ and $CrCl_2$, it was determined that the rate of depolymerization, as defined by the decrease in the degree of polymerization (DP, a measure of average glucose unit in a cellulose polymer) per minute, was 30/min, which is dramatically faster than the rate of depolymerization (3.7/min) by Brønsted-acid catalyzed cellulose depolymerization in a H_2SO_4 aqueous system [10]. Most importantly, while the DP value of the cellulose dropped from 310 to 1.9 in 30 min as a result of the paired metal chloride catalyzed hydrolysis in [EMIM]Cl, the DP value in the H_2SO_4 aqueous system only reached 96 after 60 min and the rate was further reduced thereafter. Little glucose was detected in this H_2SO_4 system even after 2 h. In the paired $CuCl_2/PdCl_2$ system, the rate of cellulose depolymerization is similar to that of the $CuCl_2/CrCl_2$ system.

We then investigated the quantities required and the specific roles played by the individual metal chlorides in the paired $CuCl_2/PdCl_2$ catalyst system. First, we systematically examined the effect of the total metal chloride loading in [EMIM]Cl solvent on the activity of paired $CuCl_2/PdCl_2$ catalysts, while keeping $\chi_{CuCl_2} = 0.90$. It was found that the total product yield did not depend linearly on the total amount of catalyst loaded. Rather, a sharp threshold was observed for catalyst loading, below which product yield was negligible. For example, with the $CuCl_2/PdCl_2$ catalysts (Fig. 2), the total yield after 1 h reaction at 120 °C was only about 2% at a total metal chloride loading of 19 μmol/g [EMIM]Cl or below. Remarkably, the yield increased to 25% at a total metal chloride loading of 25 μmol/g [EMIM]Cl and to over 70% when the total metal chloride loading was increased to 38 μmol/g [EMIM]Cl. The highest yield was observed at 55 μmol/g [EMIM]Cl total catalyst loading. Above this loading, both total and cellobiose yields decreased, likely due to product degradation due to the increased level of hydrolytic power.

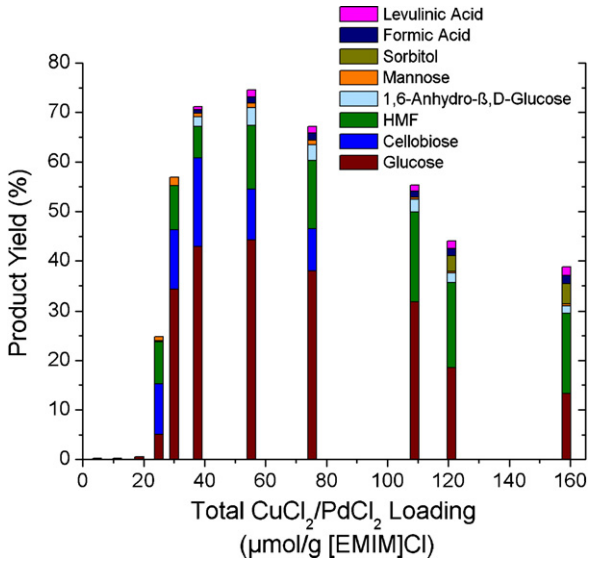

Fig. 2. Hydrolysis product yield from cellulose using paired $CuCl_2/PdCl_2$ catalyst ($\chi_{CuCl_2} = 0.09$) at different total loadings at 120 °C for 1 h. The cellulose was swelled in [EMIM]Cl at 100 °C for 1 h before adding the catalyst.

Because $CuCl_2/PdCl_2$ ($\chi_{CuCl_2} = 0.90$) was not active at a total loading of 19 μmol/g [EMIM]Cl, and was active at a total loading of 38 μmol/g [EMIM]Cl (Fig. 2), we then doubled the amount of $PdCl_2$ at the lower level (total loading 20 μmol/g [EMIM]Cl, $\chi_{CuCl_2} = 0.82$) and cut it in half at the upper level (total loading 36 μmol/g [EMIM]Cl, $\chi_{CuCl_2} = 0.95$) to identify the critical metal chloride component for the large increase in hydrolytic activity between loadings of 19 and 38 μmol/g [EMIM]Cl. We found that the catalyst activity is more sensitive to $CuCl_2$ loading in this range of metal loadings. Based on the amount of $PdCl_2$ needed to satisfy the threshold loading, the turnover number is at least 500.

To gain some insight as to the properties of the paired metal chloride catalyst in the [EMIM]Cl solvent, we characterized the system by several complementary methods. Differential scanning calorimetry (DSC) analyses of the metal chlorides in [EMIM]Cl containing dissolved cellulose (Fig. 3) yielded endothermic onset temperatures that mark the beginning of the phase conversion from solid to liquid. The DSC peak maxima, which provide a more intuitive, but less accurate, description of phase-transition behavior, and the magnitudes of the DSC heat endotherms, follow the same trend. For neat [EMIM]Cl, the onset temperature was 82.2 °C. After dissolving 10 wt.% cellulose in the [EMIM]Cl, the onset temperature dropped to 75.5 °C. Single metal chlorides, $CuCl_2$, and $PdCl_2$, in 37 μmol per gram of [EMIM]Cl (i.e., in a metal chloride/[EMIM]Cl mole ratio of 5×10^{-3}) further lowered the onset temperature by 2.3 and 2.9 °C, respectively, as compared to [EMIM]Cl containing only dissolved cellulose. While the same total metal-chloride loading was unchanged, replacing only 10% of the $CuCl_2$ (i.e., in 5×10^{-4} mol per mole of [EMIM]Cl) with an equal amount of $PdCl_2$ added to form a paired $CuCl_2/PdCl_2$ catalyst led to a substantial drop, 11.3 °C, in the endothermic onset temperature. These results suggest that the paired metal chlorides are more effective than individual metal chloride additives in disrupting the long-range bonding network between the solvent ions. Although impurities are known to lower the melting point of ionic liquids, the presence of a low concentration of single metal chlorides (in 5×10^{-3} mol per mole of [EMIM]Cl, far below the stoichoimetric amount that is typical of [EMIM]Cl·$MeCl_x$ or [EMIM]$MeCl_{x+1}$ based ionic liquids, Me = metal), induced only a moderate 1.4–2.9 °C decrease in the onset temperature. It is therefore most unusual that only 5×10^{-4} mol of $PdCl_2$ per mole of [EMIM]Cl replacing an equal amount of $CuCl_2$ from a total of 5×10^{-3} mol of paired metal chloride per mole of [EMIM]Cl caused dramatic 11.3 °C drops in endothermic onset temperature.

Table 1
EPR spectral *g*-factors and full width at half maximum (FWHM) for $CuCl_2/PdCl_2$ catalyst ($\chi_{CuCl_2} = 0.91$) at different total catalyst loadings (mol% with respect to the glucose units present in the cellulose feed).

Loading	Temp. (°C)	*g*	FWHM(g)
1.5%	25	2.12	0.70
6.0%	25	2.14	0.89
10%	25	2.14	1.31

We also applied two *in situ* spectroscopies, electron paramagnetic resonance (EPR) of Cu(II) ions and X-ray absorption fine structure (XAFS) at the Pd (24,352.6 eV) and Cu (8980.5 eV) K-edges, to probe the coordination structure, oxidation state, and rotational freedom of the metal species "at temperature" for the $CuCl_2$ and paired $CuCl_2/PdCl_2$ ($\chi_{CuCl_2} = 0.91$) catalysts in [EMIM]Cl containing 10 wt.% dissolved cellobiose or cellulose and 10 wt% H_2O. The Cu(II) EPR signals in [EMIM]Cl + 10% H_2O are considerably broader and have much lower intensities than those in pure H_2O (Fig. 4 and Table 1). These differences likely stem from significant interactions of Cu(II) ions with constituent ions of the ionic liquid and are

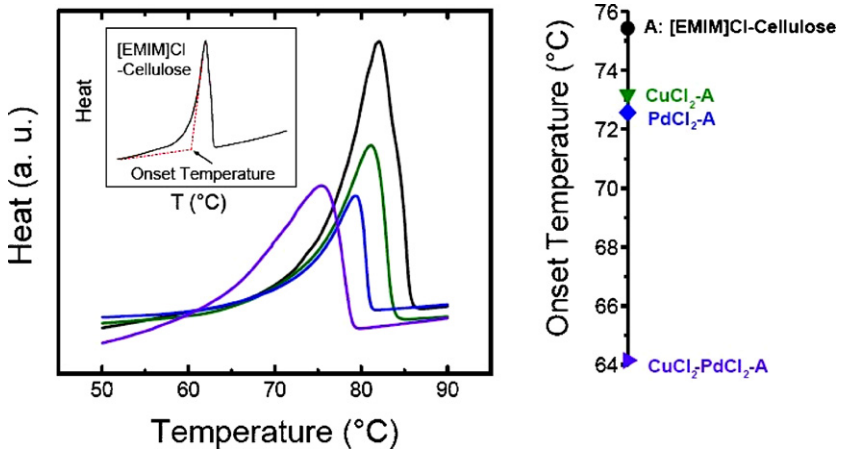

Fig. 3. Endotherms measured by differential scanning calorimetry (left) and their corresponding onset temperatures (right) for [EMIM]Cl containing 10 wt.% cellulose (A), and for this mixture to which $CuCl_2$, $PdCl_2$, or $CuCl_2 + PdCl_2$ ($\chi_{CuCl_2} = 0.91$) were added at a total metal chloride loading of 37 μmol/g [EMIM]Cl (6 mol% with respect to the glucose units present in the cellulose feed). Color of symbols on right panel indicates endotherm curves in left panel. The insert in the left panel defines the method for obtaining the onset temperature.

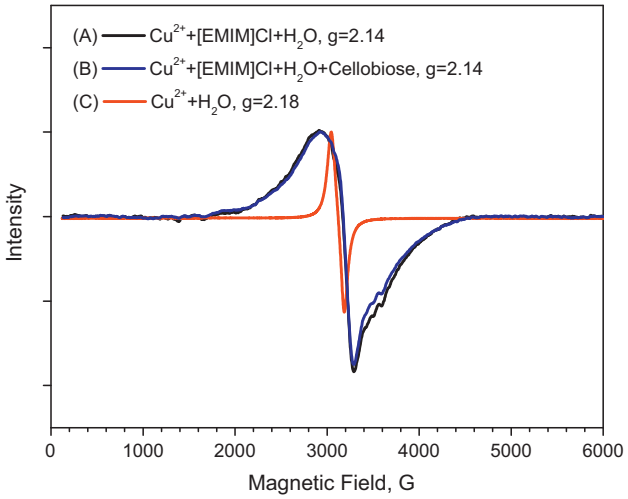

Fig. 4. (A) Cu(II) EPR spectra of $CuCl_2$ (6 mol% loading equivalent) in [EMIM]Cl containing 10 wt.% H_2O. (B) Cu(II) EPR spectra of $CuCl_2$ (6 mol% loading equivalent) in [EMIM]Cl containing 10 wt.% H_2O and 10 wt% cellobiose. (C) 0.025 M Cu(II) in aqueous solution (spectrum intensity is decreased by a factor of ~5000 for plotting purposes). All spectra collected at 20 °C.

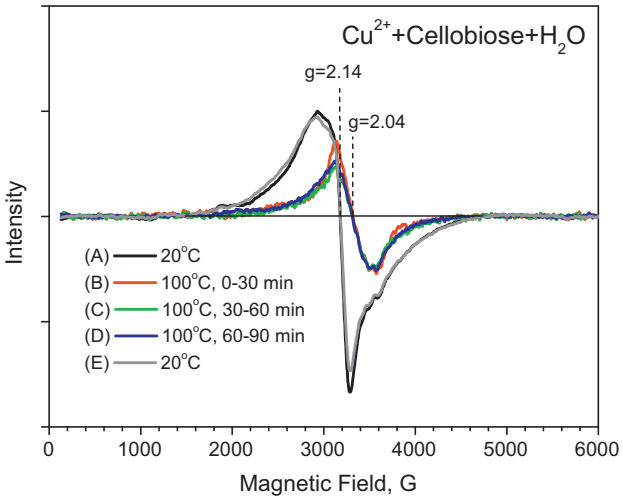

Fig. 6. Cu(II) EPR spectra of 6 mol% $CuCl_2$ in [EMIM]Cl containing 10 wt.% cellobiose and 10 wt.% H_2O. The sample was first measured at 20 °C (A) before heating to 100 °C and maintained at this temperature for up to 90 min (B–D). It was then cooled to 20 °C for another EPR measurement (E).

relatively insensitive to the presence or absence of cellobiose. XAFS results indicate that Cu(II) in [EMIM]Cl is tetrahedrally coordinated by Cl^- ions with a Cu–Cl bond distance of 2.258 Å, and a bond angle of 108° [28].

When $PdCl_2$ is added at 20 °C to substitute for 10% of the $CuCl_2$, significant differences in the Cu(II) EPR signal are obtained (Fig. 5). In the absence of Pd, the EPR signal is anisotropic, suggesting limited mobility of the Cu(II) ions. When Pd is present, an even broader, but isotropic, EPR signal is obtained. The signal broadening with Pd addition suggests greater interaction of Cu(II) with solvent and other metal ions, whereas the isotropic nature of the signal implies enhanced mobility of the Cu(II) ions in the solvent as a result of $PdCl_2$ in the ionic liquid. This interpretation is consistent with the DSC measurements suggesting decreases in long-range ionic network structure when the paired metal chlorides are present. The increased mobility of the metal ions further implies that the accessibility to cellulose by the metal ions in the [EMIM]Cl solvent is increased.

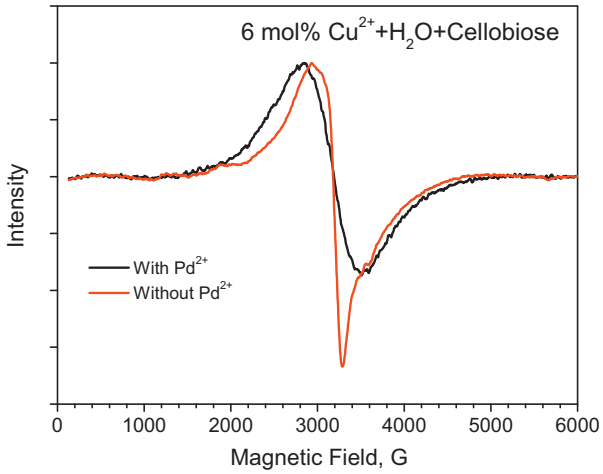

Fig. 5. EPR spectra at 20 °C of [EMIM]Cl suspensions containing 10 wt.% cellobiose, 10 wt.% H_2O, and metal chloride catalysts (total metal chloride loading is 37 μmol/g [EMIM]Cl, corresponding to 6 mol% with respect to glucose units based on cellulose feed). Curve (A) is for the paired metal catalyst $CuCl_2 + PdCl_2$ ($\chi_{CuCl_2} = 0.91$), and curve (B) is for the $CuCl_2$ catalyst alone.

Upon heating to 100 °C, the *g*-values of the EPR spectra shift to 2.04, intensities decrease due to Boltzmann effects, and nearly isotropic signals are observed in both the absence and presence of $PdCl_2$ (Figs. 6 and 7, respectively). In the absence of Pd these effects are reversible, as spectra identical to the starting spectrum are obtained upon return to room temperature (Fig. 6), indicating the oxidation state and coordination geometry of Cu(II) ions are unchanged. When Pd is present, however, the intensity of the

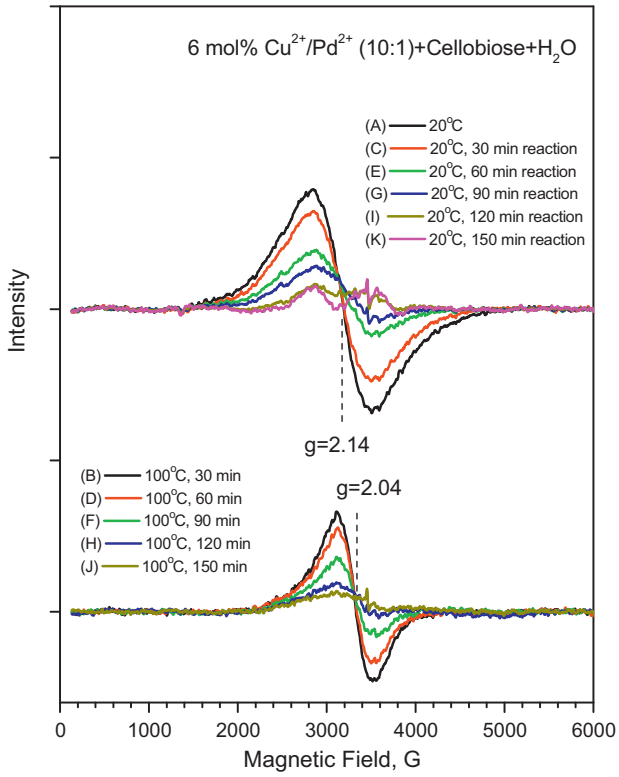

Fig. 7. Cu(II) EPR spectra of mixed $CuCl_2/PdCl_2$ with 6 mol% in total loading and $\chi_{CuCl_2} = 0.91$ in [EMIM]Cl containing 10 wt.% cellobiose and 10 wt.% H_2O. The sample was first measured at 20 °C (A) before heating to 100 °C for 30 min (B). It was then cooled to 20 °C for (C) and again heated to 100 °C (D). This procedure was repeated between 20 °C (E, G, I and K) and 100 °C (F, H and J) until a total of 150 min at 100 °C had been accumulated.

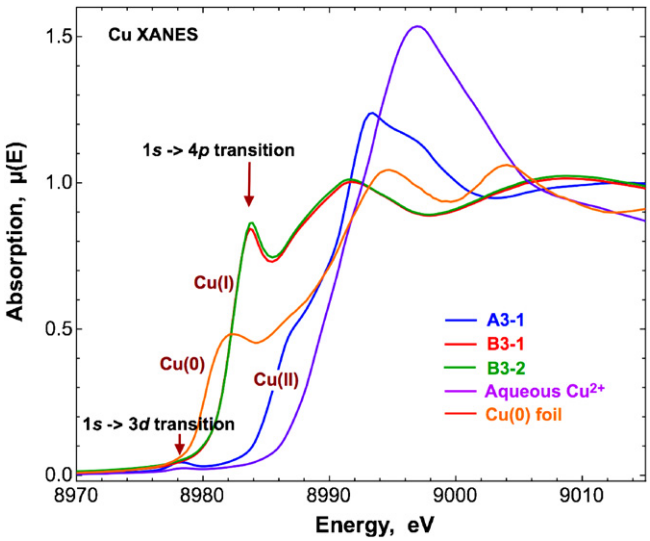

Fig. 8. X-ray absorption near edge (XANES) plots for $CuCl_2$ ( ), $CuCl_2/PdCl_2$ (and) in [EMIM]Cl containing cellulose and H_2O under various conditions. A3–1: 10% $PdCl_2$/90% $CuCl_2$, 0 wt.% cellulose, 10 wt.% H_2O, 25 °C; B3–1: 10% $PdCl_2$/90% $CuCl_2$, 10 wt.% cellulose, 10 wt.% H_2O, 25 °C; B3–2: 10% $PdCl_2$/90% $CuCl_2$, 10 wt.% cellulose, 10 wt.% H_2O, 100 °C. Before reaction, Cu(II) exists as tetrahedral $CuCl_4^{2-}$. In the presence of $PdCl_2$ and cellulose, Cu is reduced to Cu(I) that has nearly collinear Cl^- ligands. The height of the pre-edge peak is consistent with three-coordinate Cu(I) as per Kau [17].

Cu(II) signal is diminished upon return to room temperature, and, upon repeated cycling, essentially disappears irreversibly (Fig. 7). The progressive conversion of Cu(II) to an EPR-silent form, due to the presence of Pd(II) ions, is evidence for reduction to Cu(I), which is confirmed by XANES spectroscopy in the form of a strong 1s → 4p transition (Fig. 8). The theoretical fitting to the intensity of this transition in the XANES spectrum strongly suggests that Cu has three ligands. [23] The Cu(I) forms an unusual $Cl^-Cu^+–Cl^-$ structure having a Cu–Cl bond distance of 2.206 Å and a bond angle of 154°. The k^2-weighted XAFS $|\tilde{\chi}(R)|$ plots (Fig. 9) show that, during hydrolysis of the cellulose at 100 °C, the Pd(II) remains coordinated with 4 equivalent Cl^- in an isolated square-planar geometry having a Pd–Cl bond distance of 2.325 Å.

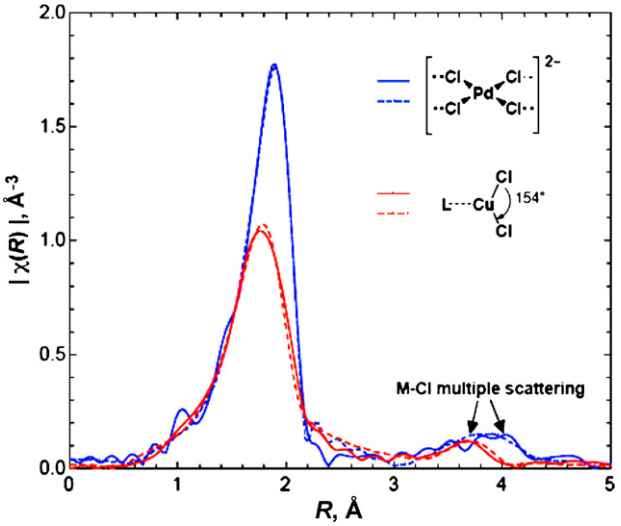

Fig. 9. The k^2-weighted $|\tilde{\chi}(R)|$ plots for the Pd and Cu catalyst species in [EMIM]Cl containing cellulose at 100 °C showing the relative distribution of Cl^- ligands about the metals. The solid lines represent the experimental values whereas the dashed lines represent the fits to the theoretical standards used to derive the structural parameters. Distances are not corrected for photoelectron phase shifts.

The identity of the L in proposed structure $LCuCl_2^-$ is unknown. On the possibility that it might be an N-heterocyclic carbene derived from removal of the C2 proton of $EMIM^+$, the structure was calculated using DFT and found to exhibit C–Cl bond distances of 2.348 Å and Cl–Cu–Cl angle of 120.5°. As a benchmark, the same level of theory finds the $CuCl_2^-$ to be linear with Cu–Cl bond distances of 2.157 Å, ~0.05 Å longer than experiment. This is consistent with computations reported by others [24]. Ligation with formate led to a structure with structural parameters similar to the NHC carbene complex with 2.37 Å for the Cu–Cl distance and sp^2-like bond angle of 124.5°. Interaction with neutral model compounds, e.g., water, formic acid, and glycol, gave structures in which O–H groups were involved in hydrogen bonds to Cl instead of ligating Cu. Interestingly, interaction of $CuCl_2^-$ with $EMIM^+$ led to deformation of the Cl–Cu–Cl angle to 169° and Cu–Cl distances of 2.14–2.16 Å. Thus, it may be that the unusual geometrical parameters observed for $CuCl_2^-$ in the reaction mixture results from interactions of $EMIM^+$ and/or weakly ligating compounds generated in the degradation of cellobiose/cellulose.

While a detailed mechanism for the unusually high activity of the paired metal chlorides for cellulose hydrolysis remains to be unveiled, the experimental evidence presented above offers some clues about the unique character of the paired metal chlorides in [EMIM]Cl solvent. The large drop in the endothermic onset temperature from the DSC measurement for the paired metal chlorides in [EMIM]Cl containing cellulose, and the broad isotropic EPR signal for $Cu(II)Cl_4^{2-}$ only in the presence of $Pd(II)Cl_4^{2-}$ point to a strong effect of the metal chloride precursors on the solvent properties and on each other. The irreversible reduction of $Cu(II)Cl_4^{2-}$ to $LCu(I)Cl_2^-$ due to the presence of $PdCl_2$, as identified by EPR and XAFS, appears analogous to the well known Wacker process [25], but unique in such a novel catalytic system. A notable difference from the Wacker chemistry in the current system is that significant effort was made to minimize oxygen in the reaction system. Based on XAFS measurements, there was no permanent reduction of Pd(II) to Pd(0) even under lean $CuCl_2$ conditions. Protons generated by hydrolysis of water may be associated with the $[PdCl_4]^{2-}$ anion that has been confirmed by XAFS measurement. Under the conditions carried out for cellulose hydrolysis, the metal ions are fully coordinated by chlorides in their unreduced states, similar to reported XAFS results on other transition metal chlorides in the form of $[EMIM]_2MeCl_4$ where Me = Mn, Co, Ni [26], as determined by XAFS. The role of $LCu(I)Cl_2^-$ in the reaction coordinate remains unclear, although we suspect it is a side reaction unrelated to the main chemistry.

We note that the product yield curve for the $CuCl_2/PdCl_2$ catalyst system differs from that reported earlier for the $CuCl_2/CrCl_3$ catalyst system [10]. When Pd is present, the maximum product yields are obtained in a broad plateau at χ_{CuCl_2} between 0.50 and 0.90 (Fig. 1), whereas when Cr(III) is present the maximum product yields are obtained in a narrow band centered at $\chi_{CuCl_2} = 0.95$. These results are consistent with the additional role of Cu(II) as an oxidant to regenerate Pd(II) in the $CuCl_2/PdCl_2$ catalyst system, in which two Cu(II) ions are needed to oxidize each Pd(0) lost to side reactions to Pd(II). Because reduction of Cr(III) is unlikely in the $CuCl_2/CrCl_3$ catalyst system, the role of Cu(II) is limited to generation of protons and alteration of the solvent structure.

We stress that the paired metal chloride catalyst system described here is quite different from the chlorometallate complexes typically described in the ionic-liquid literature. While a number of metal chlorides ($MeCl_x$) are known to form ionic liquids with [AMIM]Cl, typically in 1:1 stoichiometry resulting in [AMIM] $MeCl_{x+1}$ (mononuclear), but also with excess $MeCl_x$ in multiples (n) of the amount of [AMIM]Cl resulting in $[AMIM]Me_nCl_{nx+1}$ (polynuclear) [27], ionic liquids involving $CuCl_2$ and [EMIM]Cl have rarely been studied [10]. The very small amount of $CuCl_2$ used in our work

paired with an even smaller amount of a second metal chloride (n = 0.0005 in total) in [EMIM]Cl is a unique composition that functions as an effective catalyst for the hydrolysis of cellulose at low temperatures. At slightly higher levels of catalyst loading in the paired $CuCl_2/PdCl_2$ catalyst ($\chi_{CuCl_2} = 0.90, n_{total} = 0.007$), asymmetric Cu(II)-EPR spectra (data not shown) are obtained, in contrast to the symmetric spectra obtained for the same χ_{CuCl_2} when $n \leq 0.005$. Moreover, single metal chlorides, even at four-fold higher levels than the optimum (n = 0.020) are unable to catalyze cellulose hydrolysis under the conditions reported in this work (data not shown); a much higher reaction temperature is required. Lastly, we restate that the most active paired metal chloride catalysts also cause product degradation even at 120 °C.

Acknowledgements

This work was supported by the Laboratory Directed Research and Development Program at the Pacific Northwest National Laboratory (PNNL), a multiprogram national laboratory operated by Battelle for the U.S. DOE under contract no. DE-AC06-76RL01830. Part of the research described in this paper was performed at the Environmental Molecular Sciences Laboratory, a national scientific user facility located at PNNL. The Advanced Photon Source is supported by the U. S. Department of Energy, Office of Basic Energy Sciences, under Contract DE-AC02-06CH11357. PNC-XOR is funded by its founding institutions, the US DOE-BES, and NSERC.

References

[1] Y. Nishiyama, J. Sugiyama, H. Chanzy, P. Langan, J. Am. Chem. Soc. 125 (2003) 14300–16306.
[2] S.M. Notley, B. Pettersson, L. Wagberg, J. Am. Chem. Soc. 126 (2004) 13930–13931.
[3] Q. Gan, S.J. Allen, G. Taylor, J. Chem. Technol. Biotechnol. 80 (2005) 688–698.
[4] J.F. Saeman, Ind. Eng. Chem. Anal. Ed. 17 (1945) 35–37.
[5] N. Mosier, C. Wyman, B. Dale, R. Elander, Y.Y. Lee, M. Holtzapple, M. Ladisch, Bioresour. Technol. 96 (2006) 673–686.
[6] G. Sanchez, L. Pilcher, C. Roslander, T. Modig, M. Galbe, G. Liden, Bioresour. Technol. 93 (2004) 249–256.
[7] R.P. Swatloski, S.K. Spear, J.D. Holbrey, R.D. Rogers, J. Am. Chem. Soc. 124 (2002) 4974–4975.
[8] A. Pinkert, K.N. Marsh, S. Pang, M.P. Staiger, Chem. Rev. 109 (2009) 6712–6728.
[9] Z.C. Zhang, Adv. Catal. 49 (2006) 153–237.
[10] Y. Su, H.M. Brown, X.W. Huang, X.D. Zhou, J.E. Amonette, Z.C. Zhang, Appl. Catal. A 361 (2009) 117–122.
[11] N.S. Dalal, D.E. Kennedy, C.A. McDowell, J. Chem. Phys. 59 (1979) 3403–3410.
[12] D.C. Koningsberger, R. Prins, X-ray Absorption: Principles, Applications, Techniques of EXAFS, SEXAFS and XANES, John Wiley & Sons, New York, 1988.
[13] E.A. Stern, M. Newville, B. Ravel, Y. Yacoby, D. Haskel, Physica B 208–209 (1995) 117–120.
[14] M. Newville, P. Livins, Y. Yacoby, J.J. Rehr, E.A. Stern, Phys. Rev. B 47 (1993) 14126–14131.
[15] S.I. Zabinsky, J.J. Rehr, A. Ankudinov, R.C. Albers, M.J. Eller, Phys. Rev. B 52 (1995) 2995–3009.
[16] M. Newville, R. Ravel, D. Haskel, J.J. Rehr, E.A. Stern, Y. Yacoby, Physica B 208–209 (1995) 154–156.
[17] E.J. Bylaska, W.A. de Jong, N. Govind, K. Kowalski, T.P. Straatsma, M. Valiev, D. Wang, E. Apra, T.L. Windus, J. Hammond, P. Nichols, S. Hirata, M.T. Hackler, Y. Zhao, P.-D. Fan, R.J. Harrison, M. Dupuis, D.M.A. Smith, J. Nieplocha, V. Tipparaju, M. Krishnan, A. Vazquez-Mayagoitia, Q. Wu, T. Van Voorhis, A.A. Auer, M. Nooijen, L.D. Crosby, E. Brown, G. Cisneros, G.I. Fann, H. Fruchtl, J. Garza, K. Hirao, R. Kendall, J.A. Nichols, K. Tsemekhman, K. Wolinski, J. Anchell, D. Bernholdt, P. Borowski, T. Clark, D. Clerc, H. Dachsel, M. Deegan, K. Dyall, D. Elwood, E. Glendening, M. Gutowski, A. Hess, J. Jaffe, B. Johnson, J. Ju, R. Kobayashi, R. Kutteh, Z. Lin, R. Littlefield, X. Long, B. Meng, T. Nakajima, S. Niu, L. Pollack, M. Rosing, G. Sandrone, M. Stave, H. Taylor, G. Thomas, J. van Lenthe, A. Wong, Z. Zhang, NWChem, A Computational Chemistry Package for Parallel Computers, Version 5.1.1, Pacific Northwest National Laboratory, Richland, WA, USA, 2009.
[18] P. Hohenberg, W. Kohn, Phys. Rev. B 136 (1964) B864.
[19] W. Kohn, L.J. Sham, Phys. Rev. 140 (1965) 1133.
[20] A.D. Becke, J. Chem. Phys. 98 (1993) 5648.
[21] A. Schafer, C. Huber, R. Ahlrichs, J. Chem. Phys. 100 (1994) 5829.
[22] H. Zhao, J.E. Holladay, H. Brown, Z.C. Zhang, Science 316 (2007) 1597–1600.
[23] L.S. Kau, D.J. Spira-Solomon, J.E. Penner-Hahn, K.O. Hodgson, E.I. Solomon, J. Am. Chem. Soc. 109 (1987) 6433–6442.
[24] X.-B. Wang, L.-S. Wang, J. Chem. Phys. (2001) 7388–7395.
[25] J. Smidt, Angew. Chem. 71 (1959) 176.
[26] A.J. Dent, K.R. Seddon, T. Welton, J. Chem. Soc., Chem. Commun. (1990) 315–316.
[27] R. Rogers, K. Seddon (Eds.), ACS Symposium Series, vol. 858, American Chemical Society, Washington, DC, 2003.
[28] G. Li, D.M. Camaioni, J.E. Amonette, Z.C. Zhang, T.J. Johnson, J.L. Fulton, J. Phys. Chem. B 114 (39) (2010) 12614–12622.